

# Asymmetry of Quadratic Energy Transfer Between Ion Cyclotron and Whistler Modes in Fully Developed Hall Magnetohydrodynamic Turbulence<sup>\*)</sup>

Keisuke ARAKI and Hideaki MIURA<sup>1)</sup>

*Okayama University of Science, Okayama 700-0005, Japan*

<sup>1)</sup>*National Institute for Fusion Science, Toki 509-5292, Japan*

(Received 28 November 2019 / Accepted 4 March 2020)

This study investigated the energy transfer of a fully developed freely decaying homogeneous isotropic turbulence of a Hall magnetohydrodynamic medium from the perspective of the interaction between the ion cyclotron (IC) and whistler (Wh) modes. The variables were decomposed using generalized Elsässer variables (Galtier, *J. Plasma Phys.* **72**, 721 (2006)), which are given by a combination of velocity and magnetic fields. To analyze the energy transfer between these coupled variables, an analytical-mechanical approach was introduced that guaranteed both the Galilean covariance and the detailed energy balance for each decomposed mode. A remarkable asymmetry of the energy transfer between the IC and Wh modes was found. In the present study, almost one-sided energy transfers from the IC to the Wh modes were observed. In addition, a shell-to-shell transfer analysis revealed relatively weak inter-mode interactions with nonlocal features, while the intra-mode interactions were both intense and local.

© 2020 The Japan Society of Plasma Science and Nuclear Fusion Research

Keywords: incompressible Hall magnetohydrodynamics, generalized Elsässer variable, fully developed turbulence, energy transfer

DOI: 10.1585/pfr.15.2401024

## 1. Introduction

Among magnetohydrodynamic (MHD) models, Hall magnetohydrodynamics (HMHD) has long been investigated as a simple one-fluid MHD model that contains a two-fluid effect [1]. From the perspective of fully developed turbulence research, a wide variety of approaches have been adopted. These include wave turbulence formulation and interaction analysis [2], nonlinear energy-transfer analysis of DNS data [3], spontaneous chiral symmetry breaking [4], formation of coherent structures and comparison with those found for standard one-fluid MHD model [5], sub-grid scale modeling for LES [6], and analytical-mechanical analysis of wave/chaos timescales for homogeneous isotropic turbulence [7].

This study's authors previously identified a reduction of nonlinear interactions of the  $\mathbf{u} \times \boldsymbol{\omega}$  and  $\nabla \times (\mathbf{j} \times \mathbf{b})$  terms [8], which was later revealed to comprise part of compensating behaviors of interactions due to whole quadratic terms [9]. These results strongly suggest that the behaviors of the magnetic and velocity fields are strongly coupled. The generalized Elsässer variable (GEV) seems a plausible candidate as an analysis tool, because it was shown that the GEV is based on the analytical-mechanical structure of the HMHD, i.e., the eigenfunction of the helicity-based particle-relabeling operator, which was derived from

author's e-mail: araki@are.ous.ac.jp

<sup>\*)</sup> This article is based on the presentation at the 28th International Toki Conference on Plasma and Fusion Research (ITC28).

the consideration of system symmetry and related conservation laws [10]. By applying the GEV to the turbulence, the GEV transfer-function spectra were obtained and compared with those based on the velocity and magnetic fields [11]. However, the analysis method used had limitations in terms of the decomposition of the GEV mode. Thus, this study further elucidates the basis of mode decomposition.

This paper is organized as follows: Section 2 and 3 present explanations of the basic equations and the principal features of the GEV and the decomposition method, respectively; the mathematical foundation of the energy-transfer analysis method is reviewed in Section 4; the energy-transfer functions (ETF) decomposed according to the contribution of the ion cyclotron (IC) and whistler (Wh) components are analyzed in Section 5; Section 6 investigates the detailed energy transfer between the decomposed modes; and concluding remarks are presented in Section 7.

## 2. Basic Equations

In the HMHD system, the velocity field  $\mathbf{u}$  and the magnetic field  $\mathbf{b}$  in the normalized unit obey the following equations:

$$\partial_t \mathbf{u} + (\mathbf{u} \cdot \nabla) \mathbf{u} = -\nabla P + \mathbf{j} \times \mathbf{b} + \nu \Delta \mathbf{u}, \quad (1)$$

$$\partial_t \mathbf{b} = \nabla \times ((\mathbf{u} - \alpha \mathbf{j}) \times \mathbf{b}) + \eta \Delta \mathbf{b}, \quad (2)$$

$$\nabla \cdot \mathbf{u} = \nabla \cdot \mathbf{b} = 0, \quad (3)$$

where  $P$ ,  $\mathbf{j} := \nabla \times \mathbf{b}$ ,  $\nu$ ,  $\alpha$  and  $\eta$  are the generalized pressure, the current density field, the kinematic viscosity, the parameter specifying the relative strength of the Hall term effect, and the resistivity, respectively. In the following, the pair of the velocity and magnetic fields is denoted by  $\vec{\mathbf{Z}} := {}^t(\mathbf{u}, \mathbf{b})$  and is termed the  $\vec{\mathbf{Z}}$  variable. The basic equations (1)-(3) are symbolically denoted by

$$\partial_t \vec{\mathbf{Z}} = \vec{\mathcal{Q}}(\vec{\mathbf{Z}}, \vec{\mathbf{Z}}) + \hat{D}\vec{\mathbf{Z}}, \quad (4)$$

where  $\vec{\mathcal{Q}}$ ,  $\hat{D}\vec{\mathbf{Z}}$  are the quadratic and dissipation terms, respectively<sup>1</sup> [11].

### 3. Generalized Elsässer Variable Decomposition

The present study uses three independent methods of analysis. The first is GEV decomposition, which was discussed in detail in Section 3 of [11]. The second is the geometrically partitioned shell decomposition of the wavenumber space, which was also considered in depth in Section 3 of [8]. The third is discussed in the next section.

The GEV was first derived by Galtier [2] as the eigenfunction of the operator  $\widehat{M}$ , which appears in the following linearized problem of the basic equations (1) and (2) with a background uniform magnetic field ( $\mathbf{B}_0$ ):

$$\partial_t \vec{\mathbf{Z}} = (\mathbf{B}_0 \cdot \nabla) \widehat{M} \vec{\mathbf{Z}}, \quad \text{where} \quad \widehat{M} = \begin{pmatrix} O & I \\ I & \alpha \nabla \times \end{pmatrix}. \quad (5)$$

The equation's eigenvalues,  $\Lambda_\sigma^s(|\vec{k}|)$ , have three kinds of indices: wavenumber ( $\vec{k} \in \mathbb{Z}^3$ ), chirality ( $\sigma = \pm 1$ ), and polarity ( $s = \pm 1$ ). They are given by  $\Lambda_\sigma^s(|\vec{k}|) = \sigma s \lambda^{-s}$ , where  $\lambda = \lambda(\vec{k}) = [(\pi\alpha|\vec{k}|)^2 + 1]^{1/2} + \pi\alpha|\vec{k}|$ . The corresponding eigenfunctions,  $\vec{\Psi}_\sigma^s$ , are given by

$$\text{ion cyclotron (IC) mode: } \vec{\Psi}_\pm^+ = {}^t(\lambda\phi_\pm, \pm\phi_\pm), \quad (6)$$

$$\text{whistler (Wh) mode: } \vec{\Psi}_\pm^- = {}^t(\mp\phi_\pm, \lambda\phi_\pm), \quad (7)$$

where  $\phi_\pm = \phi_\pm(\vec{k}; \vec{x})$  are the eigenfunctions of the curl operator<sup>2</sup> ( $\nabla \times \phi_\sigma = 2\pi\sigma|\vec{k}|\phi_\sigma$ ). The mode names are chosen according to the counterpart linear waves for non-zero  $\mathbf{B}_0$ . Even when  $\mathbf{B}_0 = \mathbf{0}$ , these eigenfunctions work as orthogonal base functions of the  $\vec{\mathbf{Z}}$  variable space. The  $\vec{\mathbf{Z}}$  variable is decomposed into the GEV components as follows:

$$\vec{\mathbf{Z}} = \sum_{\vec{k}, \sigma, s} \vec{\mathbf{Z}}_\sigma^s(\vec{k}), \quad \text{where} \quad \vec{\mathbf{Z}}_\sigma^s(\vec{k}) = \frac{\langle \vec{\Psi}_\sigma^s(\vec{k}) | \vec{\mathbf{Z}} \rangle}{1 + \lambda^2} \vec{\Psi}_\sigma^s(\vec{k}),$$

where the symbol  $\langle * | * \rangle$  is the inner product defined by

$$\langle \vec{\mathbf{Z}}_1 | \vec{\mathbf{Z}}_2 \rangle := \int (\mathbf{u}_1^* \cdot \mathbf{u}_2 + \mathbf{b}_1^* \cdot \mathbf{b}_2) d^3 \vec{x}, \quad (8)$$

and the asterisk denotes a complex conjugate.

This paper focuses on the interaction between the IC

<sup>1</sup>In this paper, an arrow above a symbol denotes its multifunctional character.

<sup>2</sup>In this paper,  $\phi_\sigma$ 's are assumed to be normalized:  $\int \phi_\sigma^*(\vec{p}) \cdot \phi_\sigma(\vec{p}') d^3 \vec{x} = \delta_{\vec{p}, \vec{p}'} \delta_{\sigma, \sigma'}$ , where  $\delta$  is Kronecker's delta.

( $\vec{\mathbf{Z}}^+$ ) and the Wh ( $\vec{\mathbf{Z}}^-$ ) components, and the inter-scale interactions. Thus, the  $\vec{\mathbf{Z}}$  variable is decomposed as follows:

$$\vec{\mathbf{Z}} = \sum_{j \in \mathbb{Z}} \vec{\mathbf{Z}}_j^+ + \sum_{j \in \mathbb{Z}} \vec{\mathbf{Z}}_j^-, \quad \text{where} \quad \vec{\mathbf{Z}}_j^s := \sum_{\vec{k} \in S_j} \vec{\mathbf{Z}}_\sigma^s(\vec{k}). \quad (9)$$

In this equation, the wavenumber space partitioning shell  $S_j$  is defined by the following:

$$S_j := \{\vec{k}; 2^{-(j+1)/2} < |\vec{k}|/k_\eta(t) < 2^{-j/2}\},$$

where  $k_\eta(t) := (\epsilon_B(t)/\eta^3)^{1/4}$  is the characteristic wavenumber of the dissipation scale derived from the dissipation rate of the magnetic field:  $\epsilon_B(t) := \eta \int |\mathbf{j}(\vec{x}, t)|^2 d^3 \vec{x}$ . This partitioning method implies band-pass filtering, which is analogous to *dyadic wavelet analysis* [8, 12].

### 4. Mathematical Preliminaries for the Detailed Energy-Transfer Analysis

The third analytical method (discussed below) may seem somewhat pedantic; however, it is essential for the strict evaluation of nonlinear energy transfer.

In a previous study, the authors of this paper analyzed the evolution equation of the total energy given by

$$\frac{1}{2} \frac{d}{dt} \langle \vec{\mathbf{Z}} | \vec{\mathbf{Z}} \rangle = \langle \vec{\mathbf{Z}} | \vec{\mathcal{Q}}(\vec{\mathbf{Z}}, \vec{\mathbf{Z}}) \rangle + \langle \vec{\mathbf{Z}} | \hat{D}\vec{\mathbf{Z}} \rangle.$$

By substituting the decomposition given by Eq. (9), the decomposed energy budget equations are obtained as

$$\frac{1}{2} \frac{d}{dt} \langle \vec{\mathbf{Z}}_\pm^s | \vec{\mathbf{Z}}_\pm^s \rangle = \langle \vec{\mathbf{Z}}_\pm^s | \vec{\mathcal{Q}}(\vec{\mathbf{Z}}, \vec{\mathbf{Z}}) \rangle + \langle \vec{\mathbf{Z}}_\pm^s | \hat{D}\vec{\mathbf{Z}}_\pm^s \rangle. \quad (10)$$

The previous paper analyzed the ETFs,  $\langle \vec{\mathbf{Z}}_\pm^s | \vec{\mathcal{Q}}(\vec{\mathbf{Z}}, \vec{\mathbf{Z}}) \rangle$ , and observed the usual energy cascades to smaller scales [11]. However, as the contributions of both the IC and Wh modes to these spectra remained unresolved, further investigation was required. Nonetheless, it seems inappropriate to decompose the  $\vec{\mathbf{Z}}$  variable in the quadratic term,  $\vec{\mathcal{Q}}$ , because the resulting decomposed blocks do not satisfy the *detailed energy balance* between the decomposed modes.

To overcome the discrepancy of the previous analytical method, the differential geometrical consideration of the nature of quadratic terms was discussed in [7]. A differential-geometrical analytical-mechanical consideration of the HMHD dynamics leads to the quadratic term operator ( $\vec{\nabla}$ ), which is defined as follows:

$$\vec{\nabla} \vec{\mathbf{Z}}_1 \vec{\mathbf{Z}}_2 = \frac{1}{2} \begin{pmatrix} \omega_1 \times \mathbf{u}_2 - \mathbf{u}_1 \times \omega_2 - \nabla \times (\mathbf{u}_1 \times \mathbf{u}_2) \\ + \mathbf{b}_1 \times \mathbf{j}_2 - \mathbf{j}_1 \times \mathbf{b}_2 - \nabla P_u \\ \nabla \times (\mathbf{b}_1 \times (\mathbf{u}_2 - \alpha \mathbf{j}_2) - (\mathbf{u}_1 - \alpha \mathbf{j}_1) \times \mathbf{b}_2) \\ - \mathbf{j}_1 \times \mathbf{u}_2 - \mathbf{u}_1 \times \mathbf{j}_2 + \alpha \mathbf{j}_1 \times \mathbf{j}_2 - \nabla P_b \end{pmatrix}, \quad (11)$$

where  $\omega := \nabla \times \mathbf{u}$ ,  $P_u$ , and  $P_b$  are appropriate scalar functions to make each component divergence-free. In terms of this operator, the basic equations (Eqs. (1)-(3)) are sym-

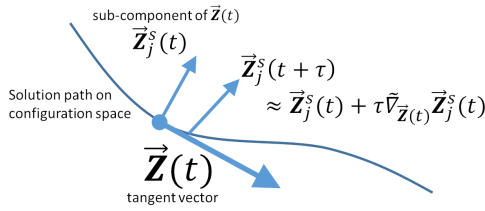


Fig. 1 A schematic view of the parallel translation of the sub-component of the generalized velocity along its solution path.

bolically denoted as  $(\partial_t + \tilde{\nabla}_{\vec{Z}})\vec{Z} = \hat{D}\vec{Z}$ .

This bizarre expression is derived from the following three physically desirable conditions [7]:

1. When  $\vec{Z}_1 = \vec{Z}_2$ , the terms are reduced to the quadratic terms of the basic equations (1) and (2):  $-\tilde{\nabla}_{\vec{Z}}\vec{Z} = \vec{Q}(\vec{Z}, \vec{Z})$ .
2. The substantial derivative of an arbitrary frozen-in vector field ( $\vec{\xi}$ ) by  $\vec{Z}$ ,  $(\partial_t + \tilde{\nabla}_{\vec{Z}})\vec{\xi}$ , is covariant against the Galilean transformation.
3. “The advection” by  $\tilde{\nabla}_{\vec{Z}}$  preserves the value of the inner product, i.e., the inner product of  $\tilde{\nabla}_{\vec{Z}}\vec{Z}$  and  $\vec{Z}$  satisfies the following:

$$\langle \tilde{\nabla}_{\vec{Z}}\vec{Z}_1 | \vec{Z}_2 \rangle + \langle \vec{Z}_1 | \tilde{\nabla}_{\vec{Z}}\vec{Z}_2 \rangle = 0. \quad (12)$$

The third condition is crucial for the energy transfer analysis because this guarantees the detailed energy balance between the two arbitrary expansion modes.

Physically, the obtained expression defines the deformation of decomposed components of the velocity and magnetic fields that retain both the Galilean covariance and energy conservation. Mathematically, the operation is a metric-preserving parallel translation, i.e., the Levi-Civita connection on configuration space (Fig. 1).

Using this expression, equation (10) is rewritten as

$$\frac{1}{2} \frac{d}{dt} \langle \vec{Z}_j^\pm | \vec{Z}_j^\pm \rangle = \sum_{l \in \mathbb{Z}} \langle j, \pm | \vec{Z} | l, s' \rangle + \sum_{s' = \pm} \langle \vec{Z}_j^\pm | \hat{D}\vec{Z}_j^\pm \rangle, \quad (13)$$

where the symbol  $\langle * | * | * \rangle$  is defined by

$$\langle j, \pm | \vec{Z} | l, s' \rangle := -\langle \vec{Z}_j^\pm | \tilde{\nabla}_{\vec{Z}}\vec{Z}_l^{s'} \rangle, \quad (14)$$

and is referred to as a shell-to-shell ETF hereafter. The values of shell-to-shell ETF satisfy the detailed energy-balance condition:

$$\langle j, s | \vec{Z} | l, s' \rangle = -\langle l, s' | \vec{Z} | j, s \rangle. \quad (15)$$

Due to this relationship, the energy budgets between the arbitrary pair of the  $(j, s)$ - and  $(l, s')$ -modes balance each other:

$$\begin{aligned} \frac{d}{dt} \langle \vec{Z}_j^s | \vec{Z}_j^s \rangle &= \dots + \langle j, s | \vec{Z} | l, s' \rangle + \dots, \\ \frac{d}{dt} \langle \vec{Z}_l^{s'} | \vec{Z}_l^{s'} \rangle &= \dots + \langle l, s' | \vec{Z} | j, s \rangle + \dots. \end{aligned}$$

Thus, the meaning of the symbol  $\langle j, s | \vec{Z} | l, s' \rangle$  is the energy transfer *from* the  $(l, s')$ -mode *to* the  $(j, s)$ -mode due to *ad-*

*vection* by the plasma motion  $\vec{Z}$ . In the following, the  $|l, s'\rangle$  side is referred to as the from (F) mode and the  $\langle j, s|$  side as the to (T) mode.

Note that the sum of the shell-to-shell ETF overall scale index ( $l$ ) and wave mode ( $s$ ) satisfies the following:

$$\sum_{l \in \mathbb{Z}} \langle j, \pm | \vec{Z} | l, s' \rangle = \langle \vec{Z}_j^\pm | \vec{Q}(\vec{Z}, \vec{Z}) \rangle, \quad (16)$$

the right-hand side of which was previously analyzed in [11]. Therefore, this paper’s principal research objective is the detailed analysis of the decomposed modes in the left hand side of this formula.

## 5. Contribution of Ion Cyclotron and Whistler Modes to Energy Transfer

This study analyzes the same DNS datasets used in [8], [9], and [11], in which the basic properties of the analyzed turbulence fields were reported. To enable a suitable comparison, the physical quantities of the different time snapshots of the freely decaying turbulence are normalized them using the dissipation rate of the magnetic field of each snapshot  $\epsilon_B(t)$  and the resistivity  $\eta$ .

First, the decomposition of the ETF of the IC (+) and Wh (–) modes,  $\langle \vec{Z}_j^\pm | \vec{Q}(\vec{Z}, \vec{Z}) \rangle$ , into the contributions *from* the IC and Wh modes was investigated. The decomposition is given by  $\langle \vec{Z}_j^s | \vec{Q}(\vec{Z}, \vec{Z}) \rangle = \langle j, s | \vec{Z} | + \rangle + \langle j, s | \vec{Z} | - \rangle$ , where the ETF for the  $s'$ -modes are defined by

$$\langle j, s | \vec{Z} | s' \rangle := \sum_{l \in \mathbb{Z}} \langle j, s | \vec{Z} | l, s' \rangle, \quad (17)$$

for  $s, s' = \pm 1$ . In Fig. 2 the ETF for  $1 \leq t \leq 5$  are shown in terms of their time evolution.

It is remarkable that the nonlinear energy transfer between the IC and Wh modes ( $\langle j, - | \vec{Z} | + \rangle$  and  $\langle j, + | \vec{Z} | - \rangle$ ) is quite asymmetric (Figs. 2 (b) and (c)). In this case, almost one-sided energy transfers from the IC to the Wh modes are observed. In particular, the Wh modes are excited for almost all wavenumber ranges due to the interactions between both modes.

Conversely, those between the same wave modes ( $\langle j, s | \vec{Z} | s \rangle$  for  $s = \pm$ ) have similar energy-transfer profiles which indicate usual energy cascades to smaller scales (Figs. 2 (a) and (d)).

It should be noted that such asymmetry was neither observed for the bulk ETF,  $\langle \vec{Z}_j^s | \vec{Q}(\vec{Z}, \vec{Z}) \rangle$ , (see the lower two panels of Fig. 3 in [11]), nor the the ETF for  $\mathbf{u}$  and  $\mathbf{b}$  (see Fig. 4 of [8]).

The orders of magnitude of energy transfer, i.e., the significant values of the ETF, are roughly about  $0.01\epsilon_B(t) \sim 0.1\epsilon_B(t)$ , irrespective of the wave mode species. Energy is transferred between the Fourier shells and the wave mode components at comparable magnitudes.

It is interesting that the evolution of IC-to-IC ETF,  $\langle j, + | \vec{Z} | + \rangle$ , reveals that somewhat weak inverse energy transfer at the large scale components ( $|\vec{k}| \sim 0.03k_\eta$  of Fig. 2 (a)) gradually grows over time. However, such trans-

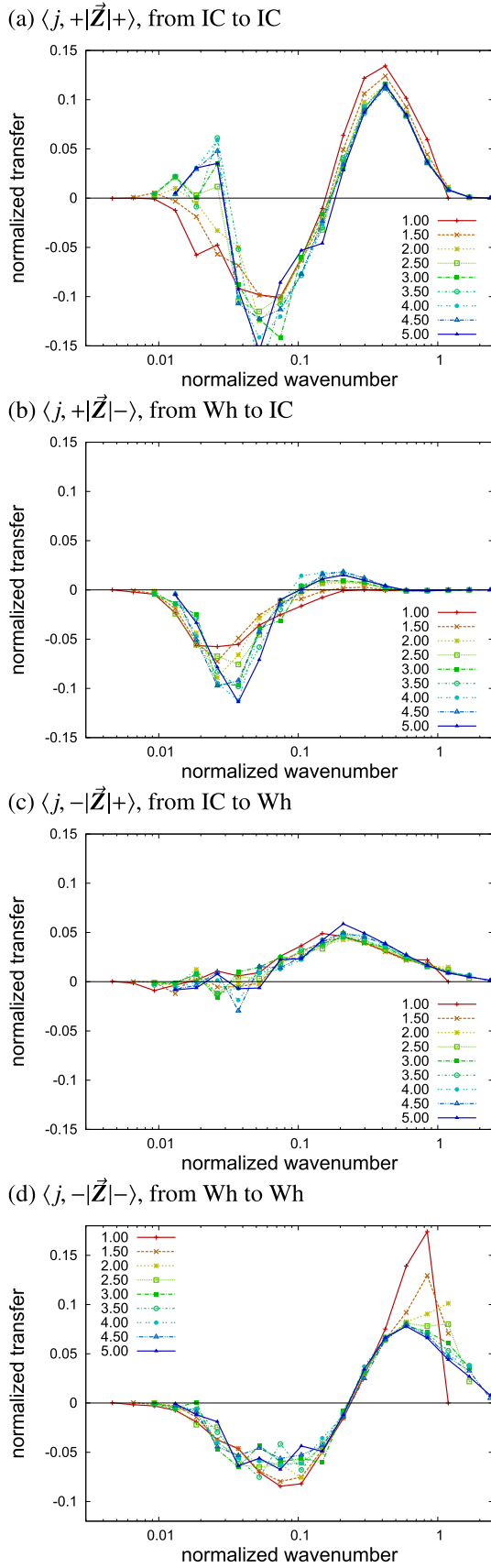


Fig. 2 Time series of the ETF spectra for each wave mode,  $\langle j, s|\vec{Z}|s' \rangle$  for  $s, s' = \pm 1$ : Both the moduli and abscissa are normalized using  $\epsilon_B(t)$  and  $\eta$ .

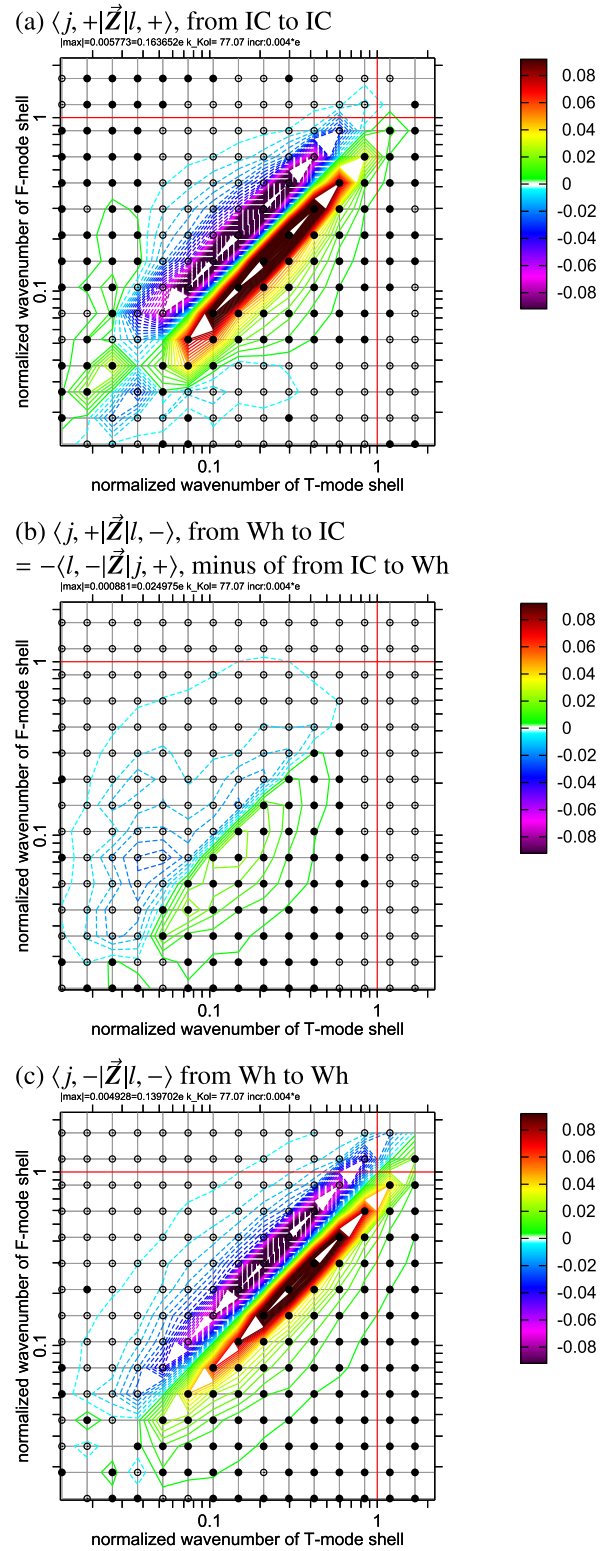


Fig. 3 Shell-to-shell ETF at  $t = 5$ :  $\langle j, s|\vec{Z}|l, s' \rangle$ . Abscissa: T-mode shell ( $\langle j, s \rangle$ ), ordinate: F-mode shell ( $\langle l, s' \rangle$ ). Contours are drawn to intuitively represent their amplitude: green to red indicates energy gain, while blue to purple indicates energy loss. The contour increment of contours is set at  $0.004\epsilon_B(t)$ . The unit of measurement of the color legend bar is  $\epsilon_B(t)$ . Normalized wavenumbers are shown at the abscissa and ordinate.

fers to larger scales were not detected for the analysis of the Wh-to-Wh ETF or the bulk ETF,  $\langle \vec{Z}_j | \vec{Q}(\vec{Z}, \vec{Z}) \rangle$  [11].

## 6. Inter- and Intra-Mode Shell-to-Shell Energy Transfer

The decomposition of the bulk ETF into the contributions of the IC and Wh modes ( $\langle j, s | \vec{Z} | s' \rangle$ ) reveals very interesting features of mode interaction, while the analysis of the shell-to-shell ETF  $\langle j, s | \vec{Z} | l, s' \rangle$  is necessary to elucidate the time evolution of the energy budget of each of the  $(j, s)$ -modes.

First, it is remarkable that the same mode interaction (IC-to-IC and Wh-to-Wh) are significantly more intense than those between different modes (IC-to-Wh). The largest moduli of the IC-to-IC and Wh-to-Wh ETF are  $0.16\epsilon_B(t)$  and  $0.14\epsilon_B(t)$ , respectively, while the modulus of IC-to-Wh one is  $0.025\epsilon_B(t)$ .

In addition, both the IC-to-IC and Wh-to-Wh ETF exhibit very sharply aligned peaks on the  $j = l \pm 1$  lines (Figs. 3 (a) and (c)). Physically this implies that the energy in an observed scale is transferred from and to the nearest spatial scale components, i.e., the local interactions in terms of wavenumber space are dominant in the transfer processes between the same wave modes.

This indicates that the principal turbulent energy-transfer process is the energy cascade to smaller scales up to dissipation scales. This has quite similar features to the fully developed turbulence in a neutral fluid [13], which suggests that if dissipation is weak, the energy cascade between the IC-modes is reachable at small scales up to kinetic scales.

These energy bucket brigades between the nearest shells result in considerable cancellations of the shell-to-shell ETF and produce moderate ETF values; this has long been known for fully-developed homogeneous isotropic turbulence of a neutral fluid [13].

Conversely, the significant values of the IC-to-Wh ETF, which are related to the Wh-to-IC ETF by Eq. (15), are distributed to rather broader areas, i.e., relatively non-local features are shown (Fig. 3 (b)).

Despite its relatively small value size, the cancellation of the IC-to-Wh ETF associated with summing up with respect to F-modes are also small; therefore, the order of magnitude of the IC-to-Wh ETF become close to those of the IC-to-IC or the Wh-to-Wh modes.

Another remarkable feature of the shell-to-shell IC-to-Wh ETF is that their moduli take large values at relatively small wavenumber regions, i.e., the dominant interactions between the IC and Wh modes occur at larger spatial scales. Conversely, smaller-scale motions of the IC and Wh modes gradually become less influential each other.

One possible explanation is as follows. Applying Eq. (5), the characteristic frequencies of the IC ( $\vec{p}$ ) and Wh ( $\vec{q}$ ) modes are roughly estimated by  $|\mathbf{b} \cdot \vec{p}|/\lambda(p)$  and  $|\mathbf{b} \cdot \vec{q}|/\lambda(q)$ , respectively. Assuming both that dominant in-

teractions are local,  $p \sim q$ , which implies  $\lambda(p) \sim \lambda(q)$ , and that they occur when these modes have close timescales,  $|\mathbf{b} \cdot \vec{p}|/\lambda(p) \sim |\mathbf{b} \cdot \vec{q}|/\lambda(q)$ , the wavenumber vectors satisfy the relationship

$$\left| \frac{\mathbf{b} \cdot \vec{p}}{\mathbf{b} \cdot \vec{q}} \right| \sim \lambda(p)\lambda(q) > 1.$$

Considering that  $\lambda(p) = [1 + (\pi\alpha p)^2]^{1/2} + \pi\alpha p$  monotonically increases with respect to  $p$ , this interaction condition is satisfied only when  $|\mathbf{b} \cdot \vec{q}|$  is sufficiently small, i.e., the wavenumber vector of the Wh mode,  $\vec{q}$ , is almost perpendicular to the ambient magnetic field,  $\mathbf{b}$ , as the wavenumbers increase. This assumes that it becomes more difficult to satisfy the resonant interaction conditions between these modes. Thus, the dynamics of the IC and Wh modes become more independent as the spatial scales of the field structures decrease.

## 7. Discussion

This study investigates the energy-transfer process from the perspective of the interaction between the IC and Wh modes. A remarkable asymmetry of the ETF between both modes is observed, while their order of magnitudes is comparable. Further decomposition into the shell-to-shell ETF revealed that the interactions between the same wave modes are intense and local, while those between the IC and Wh modes are relatively weak and nonlocal and occur at larger spatial scales.

These features suggest that, because of the deviation of the characteristic timescales between the IC and Wh modes at greater wavenumbers (i.e., at smaller spatial scales), the Hall term effect reduces the mutual dependence of the plasma fluid motion and magnetic field dynamics at smaller scales.

It is noteworthy that this dynamic splitting feature is independent of the sign of chirality; this is because one of the basic features of GEV decomposition is that, when the parity reversal transformation is applied to  $\vec{Z}_{\sigma}^s$ , it is transformed to the same wave mode with the opposite chirality sign:  $\vec{Z}_{\sigma}^s \rightarrow \vec{Z}_{-\sigma}^s$ .

The last section of this paper outlines an assumption to explain the asymmetry of the interaction between the IC and Wh modes.

Using the following three-mode truncated model,<sup>3</sup> triad interaction (see [14]) is considered, i.e., the energy transfer between the assigned three GEV modes ( $\vec{k} + \vec{p} + \vec{q} = \vec{0}$ ):

$$\begin{cases} \dot{Z}_k^* = (\Lambda_q - \Lambda_p)T_{kpq}Z_pZ_q, \\ \dot{Z}_p^* = (\Lambda_k - \Lambda_q)T_{kpq}Z_qZ_k, \\ \dot{Z}_q^* = (\Lambda_p - \Lambda_k)T_{kpq}Z_kZ_p, \end{cases} \quad (18)$$

where  $k$ ,  $p$ , and  $q$  stand for the indices of the GEV modes (e.g.  $k = (\vec{k}, \sigma_k, s_k)$ ,  $\Lambda_k = \Lambda_k^{s_k}(|\vec{k}|)$ ) [15].

<sup>3</sup>In this paper, the totally antisymmetric tensor  $T_{kpq}$  is defined by  $T_{kpq} := 2\langle \vec{Z}_k | \vec{\nabla}_{Z_p} \vec{Z}_q \rangle / (\Lambda_p - \Lambda_q - \Lambda_k)$  (cf. Ref. [7], Appendix C).

This model has two constants of motion, the energy  $E$  and the modified cross helicity  $H$  [10, 16]:

$$E = E_k + E_p + E_q, \quad (19)$$

$$H = \Lambda_k E_k + \Lambda_p E_p + \Lambda_q E_q, \quad (20)$$

where  $E_j = \frac{1}{2}|Z_j|^2$  ( $j = k, p, q$ ). Supposing that the energy of each mode varies as  $E_j \rightarrow E_j + \delta E_j$ , the variations ( $\delta E_j$ ) satisfy the following two equations:

$$\delta E_k + \delta E_p + \delta E_q = 0, \quad (21)$$

$$\Lambda_k \delta E_k + \Lambda_p \delta E_p + \Lambda_q \delta E_q = 0, \quad (22)$$

which are solved as follows:

$$\delta E_k = -\frac{\Lambda_q - \Lambda_p}{\Lambda_q - \Lambda_k} \delta E_p, \quad \delta E_q = -\frac{\Lambda_p - \Lambda_k}{\Lambda_q - \Lambda_k} \delta E_p. \quad (23)$$

Suppose that  $\Lambda_k < \Lambda_p < \Lambda_q$ , the lowest ( $k$ ) and highest ( $q$ ) modes acquire energies, i.e.  $\delta E_k, \delta E_q > 0$ , when the medium mode ( $p$ ) supplies energy,  $\delta E_p < 0$ . Conversely, remember that the eigenvalues of the GEV modes satisfy the following inequality:

$$\Lambda_{\mp}^- < -1 < \Lambda_{\mp}^+ < 0 < \Lambda_{\mp}^+ < 1 < \Lambda_{\mp}^-, \quad (24)$$

for arbitrary IC modes ( $\Lambda_{\sigma}^+$ ) and Wh modes ( $\Lambda_{\sigma}^-$ ) irrespective of their wavenumbers. This implies that the Wh mode must become the highest or lowest modes of the triad interaction between the IC- and Wh-modes. Thus, the Wh-modes seem to have more potential for energy acquisition than the IC modes; certainly, this requires further analysis in a future study. This relationship plausibly explains that energy transfers mainly from the IC to Wh modes.

## Acknowledgments

The authors appreciate the helpful comments of an anonymous referee, which greatly contributed to improving the consideration of physical processes. This work was performed under the auspices of the NIFS Collaboration Research Program (NIFS19KNSS123) and KAKENHI (Grant-in-Aid for Scientific Research(C)) 23540583.

- [1] M.J. Lighthill, *Philos. Trans. R. Soc. Lond. A*, **252**, 397 (1960).
- [2] S. Galtier, *J. Plasma Phys.* **72**, 721 (2006).
- [3] P.D. Mininni, A. Alexakis and A. Pouquet, *J. Plasma Phys.* **73**, 377 (2007).
- [4] R. Meyrand and S. Galtier, *Phys. Rev. Lett.* **109**, 194501 (2012).
- [5] H. Miura and K. Araki, *Phys. Plasmas* **21**, 072313 (2015).
- [6] H. Miura, K. Araki and F. Hamba, *J. Comput. Phys.* **316**, 385 (2016).
- [7] K. Araki, *J. Phys. A: Math. Theo.* **50**, 235501 (2017).
- [8] K. Araki and H. Miura, *Plasma Fusion Res.* **8**, 2401137 (2013).
- [9] K. Araki and H. Miura, *Plasma Fusion Res.* **9**, 3401073 (2014).
- [10] K. Araki, *Phys. Rev. E* **92**, 063106 (2015).
- [11] K. Araki and H. Miura, *Plasma Fusion Res.* **10**, 3401030 (2015).
- [12] C.K. Chui, *An introduction to wavelets* (Academic Press, London, 1992) Chapt. I.
- [13] J.A. Domaradzki and R.S. Rogallo, *Phys. Fluids A* **2**, 413 (1990).
- [14] F. Waleffe, *Phys. Fluids A* **4**, 350 (1992).
- [15] K. Araki, arXiv:1601.05477v2
- [16] K. Araki, *J. Phys. A: Math. Theo.* **48**, 175501 (2015).